EFDA–JET–PR(12)22

P. Migliano, P. Mantica, B. Baiocchiy, A.Casati, C. Giroud,
N. Hawkes, E. Lerche, M. Tsalas, D. Van Eester
and JET EFDA contributors

The Dependence of Ion Heat Transport on the Ion to Electron Temperature Ratio in JET Non-Rotating Plasmas

The Dependence of Ion Heat Transport on the Ion to Electron Temperature Ratio in JET Non-Rotating Plasmas

P. Migliano[1,2], P. Mantica[2], B. Baiocchiy[3], A.Casati[4], C. Giroud[5], N. Hawkes[5], E. Lerche[6], M. Tsalas[7], D. Van Eester[6] and JET EFDA contributors*

JET-EFDA, Culham Science Centre, OX14 3DB, Abingdon, UK

[1]Universita degli Studi di Milano Bicocca, Dept. of Physics, Milano, Italy
[2]Istituto di Fisica del Plasma 'P.Caldirola', Associazione Euratom-ENEA-CNR, Milano, Italy
[3]Universita degli Studi di Milano, Dept. of Physics, Milano, Italy
[4]Association Euratom-CEA, CEA/IRFM, F-13108 Saint Paul Lez Durance, France
[5]EURATOM-CCFE Fusion Association, Culham Science Centre, OX14 3DB, Abingdon, OXON, UK
[6]LPP-ERM/KMS, Association Euratom-Belgian State, TEC, B-1000 Brussels, Belgium
[7]FOM Institute Rijnhuizen, Association EURATOM-FOM, Nieuwegein, The Netherlands
** See annex of F. Romanelli et al, "Overview of JET Results",*
(23rd IAEA Fusion Energy Conference, Daejon, Republic of Korea (2010)).

Preprint of Paper to be submitted for publication in
Plasma Physics and Controlled Fusion

ABSTRACT

Detailed experimental studies of ion heat transport have been carried out in JET to explore the T_e/T_i dependence of ion heat transport in ITER relevant range of parameters ($T_e/T_i \geq 1$) using low rotation plasmas with dominant ion cyclotron resonance heating (ICRH) to avoid the coupling of the effects of T_e/T_i and rotation which affected previous experiments. This experimental set up has led to an accurate determination of the ion temperature gradient (ITG) threshold at varying T_e/T_i, offering unique opportunities for validation of the well-established theory of ITG driven modes. A rather mild decrease of threshold with increasing T_e/T_i in the interval of ITER interest was found. The new experimental result has found good agreement with theoretical predictions based on quasi-linear fluid and linear gyro-kinetic models.

1. INTRODUCTION

The heat fluxes observed experimentally in tokamak plasmas are 1-2 orders of magnitude higher than those that can be ascribed to collisions. The dominant mechanism of this anomalous transport are turbulent phenomena. This paper focuses on the study of electrostatic micro-instabilities due to the presence of an Ion Temperature Gradient (ITG). There is a critical value of the normalized inverse temperature gradient length $R/L_{Ti} = R|\nabla T_i| = T_i$ (with R the tokamak major radius) above which ITG modes become unstable [7]-[10] so ITGs feature a threshold in R/LT_i above which the ion heat flux (q_i) increases strongly with R/L_{T_i}. This property leads to stiffness of T_i profiles with respect to changes in heating proles. The level of stiffness characterizes how strongly T_i profiles are tied to the threshold.

The role of T_e/T_i on ion heat transport has been extensively investigated theoretically [10]-[15] and experimentally [1]-[5]. The ITG threshold value is thoretically predicted to decrease with increasing T_e/T_i and with decreasing s/q (with s magnetic shear and q safety factor) [8] [10] [11] [13], whilst the effect of rotation results mainly in a threshold up-shift according to the well known Waltz quenching rule [16]. Previous experiments on tokamaks DIII-D, ASDEX-Upgrade and JET [1]-[5] have shown a strong deterioration in both ion and electron confinement with increasing ratio T_e/T_i. All these experiments were however performed in high rotation plasmas, in which a correct determination of the pure dependence of transport on T_e/T_i is problematic because of concomitant variations of rotation and T_e/T_i. In [5] the need to take into account the concomitant effect of T_e/T_i and rotational shear was recognized. Unfortunately, the two parameters were strongly coupled in the experiments, and the effect of each could not be experimentally separated. An attempt was made to estimate the contribution of the rotational shear using linear GS2 simulations. However, this was made assuming a E×B shear threshold up-shift from the Waltz rule, which according to recent JET findings is an underestimate of the rotation effect [19] [20]. Furthermore, all these studies were performed in the range $T_e/T_i \leq 1$ which together with the presence of rotation, severely limits the reliability of the extrapolations to the predictions of ITER performances. In fact, in future reactors, because of the dominant electron heating a ratio $T_e/T_i \leq 1$ is expected. It is therefore important to understand the parametric dependence of transport on T_e/T_i in the range $T_e/T_i \leq 1$ and avoiding the coupling with concomitant variations of rotation.

The aim of this paper is to study the dependence of turbulent ion heat transport due to ITG modes on T_e/T_i in plasmas with dominant Ion Cyclotron Resonance Heating (ICRH) and therefore low rotation and in the range of interest for ITER, and compare the experimental observations with theory based models expanding the range of investigation of T_e/T_i compared to previous studies.

The paper is organized as follows: in section 2 we present the main experimental observations; in section 3 the modelling is performed and its results are compared with the experimental observations; summary and conclusions are drawn in section 4.

2. EXPERIMENTAL OBSERVATIONS

The ITG threshold at a chosen radial location is determined experimentally by the measure of R/L_{T_i} when the local ion heat flux (q_i) is close to zero. Small values of core qi are achievable with off-axis heating, which however prevents significant variations of the value of T_e/T_i in the central zone of the plasma. A good variation of T_e/T_i is obtained instead by applying the ICRH or LH (Lower Hybrid) power centrally, using different absorption schemes to change the power repartition on the electron and ion species. In this situation of necessarily high core ion heat flux, the measure of the threshold is only possible in conditions of very stiff transport, which keeps the ion temperature prole near threshold also in the presence of high heat fluxes, making the extrapolation to zero flux more reliable. Recent JET results on ion stiffness [19] [20] indicated that low rotation plasmas exhibit highly stiff ion heat transport. Therefore ICRH heated, low rotation plasmas are the ideal plasmas for the study of the effects of T_e/T_i on ITG threshold. At high rotation instead the level of ion stiffness is small, the plasma stays well above threshold and the extrapolation to the threshold value would require a detailed knowledge of the stiffness level, which appears to be strongly influenced by variations of the rotation. For the low rotation experiments in JET, it was possible to vary the value of T_e/T_i in the range $1 < T_e/T_i < 1.6$ using the ICRH heating and in the range $1.2 < T_e/T_i < 2.4$ with the LH heating. Therefore a reliable measurement of the dependence of the ITG threshold on T_e/T_i for $T_e/T_i > 1$ was obtained. The range $T_e/T_i < 1$ is not accessible in low rotation plasma due to the smaller stiffness of electrons compared to ions (which makes very effective the small residual Ohmic power even in presence of dominant ion heating onto stiff ions), but on the other hand, it is of minor relevance for ITER operations.

2.1 EXPERIMENTAL SET-UP

The JET tokamak (R = 2.96 m, a = 1m) [17] is equipped with high quality active charge exchange spectroscopy (CX) [18] for ion temperature (T_i) and toroidal rotation (ω_t) measurements and a multi-frequency ICRH for flexible and fairly localized ion heating using (^{3}He)-D minority scheme [6]. These tools, together with JET's large size and low normalized ion gyro-radius, make it an ideal device to perform detailed ion transport studies.

The ion transport experiments were all performed in low triangularity JET L-mode plasmas with $B_T = 3.36$T, $I_p = 1.8$MA, $n_{e0} \approx (2\text{-}3) \times 10^{19}$ m^{-3}. In this paper we investigate the parametric dependences of ion threshold on T_e/T_i using only low rotation plasmas and relying on the observation

that at low rotation ions are stiff, so the actual measure of R/L_{T_i} even for on-axis ICRH gives a good approximation of the threshold value.

In JET, scans of T_e/T_i at similar q (safety factor) prole ($s \approx 0.5$ at $\rho_{tor} = 0.33$, figure 1b shows q radial proles for three representative discharges) were carried out at low rotation, using central ICRH deposition and varying the thermal power partition between ions and electrons by changing minority species and its concentration: from dominant electron in 3% (H)-D minority to dominant ion in 7% (^{3}He)-D to dominant electron in 20% (^{3}He)-D where mode conversion takes place. This led to a range in T_e/T_i at $\rho_{tor} = 0.33$ from 1 to 1.6 (figure 1a shows ion and electron temperature radial proles for two representative discharges). To extend this range, previous experimental JET data in L-mode plasmas with $B_T = 3T$, $I_p = 1.3MA$, $n_{e0} \approx 2 \times 10^{19}$ m^{-3} and pure electron heating by LH were also considered, providing an excursion of T_e/T_i from 1.2 to 2.4 at $\rho_{tor} = 0.33$, although not being a fully homogeneous dataset with the main one with respect to machine conditions and main plasma parameters, including the q prole shape, due to the presence of LH current drive. It is important to note that due to the very high ion stiffness at low rotation, it is experimentally impossible to produce low rotation plasmas with $T_e/T_i < 1$, since adding ion power does not increase R/L_{T_i} and on the other hand the mere Ohmic power is sufficient to heat electrons at a similar level given their much lower stiffness level.

Values of R/L_{T_i} from the CX diagnostics [18] (time resolution: 10ms, width of probed volume ≈6cm, 12 channels, uncertainty on T_i: ±5%, on ω_t: ±8%) were obtained by linear best fit of $\log(T_i)$ data for a given selection of channels, after having time averaged the T_i measurements over a stable interval. The uncertainty on R/L_{T_i} is then estimated by repeating such procedure for different time intervals and different combinations of channels and evaluating the deviation in the set of R/L_{T_i} values so obtained. Error bars are typically $\Delta R/L_{T_i} \approx \pm 0.3$-$0.6$. R/L_{T_i} is calculated with respect to the flux surface minor radius $\rho = (R_{out} - R_{in})=2$, where R_{out} and R_{in} are the outer and inner boundaries of the flux surface on the magnetic axis plane. The values of q_i for ICRH shots have been calculated using the PION [22] code for ICRH and the PENCIL [23] code for NBI (Neutral Beam Injection). For our conditions the uncertainty on the ion thermal power deposited within $\rho_{tor} = 0.33$ is estimated ≈100kW, which typically corresponds to $\Delta q_i^{GB} \approx \pm 2$-$3$. The safety factor (q) profiles have been reconstructed by MSE. The statistical error on the value of the magnetic shear (s) is estimated to be $\approx \pm 0.05$. n_e and T_e were measured by LIDAR or high resolution Thomson scattering (HRTS) and T_e also by ECE radiometer (figure 1b shows electron density radial profiles for two representative discharges). Uncertainties are typically 5% for Te and 10% for n_e with HRTS, larger with LIDAR.

2.2 EXPERIMENTAL RESULTS

Heat fluxes are predicted by theory to follow a gyro-Bohm scaling, so that q_i can be written in a general way as [21]

$$q_i = q_i^{res} + n_i q^{1.5} \chi_s \frac{T_i^2 \rho_i}{eBR^2} \frac{R}{L_{Ti}} f \left[\frac{R}{L_{Ti}} - \frac{R}{L_{Ti_{crit}}} \right] \cdot H \left[\frac{R}{L_{Ti}} - \frac{R}{L_{Ti_{crit}}} \right], \qquad (1)$$

where q_i^{res} is the residual flux, including the neoclassical flux, n_i the ion density, q the safety factor, B the magnetic field, e the electron charge, $\rho_i = (m_i T_i)^{1/2}/eB$, m_i the ion mass, and H the Heaviside function. Equation (1) will be referred to in the following as critical gradient model (CGM), $R/L_{Ti_{crit}}$ as threshold and s as stiffness coefficient. From the curve of the gyro-Bohm normalized flux q_i^{GB} versus R/L_{Ti}, the threshold can be identified as the intercept at neoclassical flux and the stiffness coefficient can be inferred from the slope. This implies a normalization of qi over a factor $n_i q^{1.5} T_i^{5/2}/R^2 B^2$. In this paper $f(R/L_{Ti})$ is assumed linear, so q_i is quadratic in R/L_{Ti}.

The results are summarized in figures 2-5. Figure 2 shows the calculated q_i^{GB} versus the measured R/L_{Ti} at $\rho_{tor} = 0.33$ for the ICRH shots at low rotation (red full circles). For comparison, in some discharges NBI power has been added, inducing rotation at two different levels (medium rotation: blu full triangles, high rotation: black full squares). One can see the significant increase of R/L_{Ti} in rotating plasmas, which was interpreted in [19] as due to decreased stiffness due to rotation and low s. Such dependences of stiffness on rotation and s completely mask the T_e/T_i dependence of threshold. In addition, in these plasmas, due to dominant NBI heating, $T_e/T_i < 1$ and it is not possible to increase it because electrons become stiff and ions non-sti. Therefore, rotating plasmas are for these reasons of little use to study the effects of T_e/T_i on ITG threshold in ITER relevant conditions.

At low rotation, one can see that ion stiffness is very high, and therefore the measured R/L_{Ti} is already a good estimate of threshold. An even better estimate can be achieved for the ICRH shots by assuming that the same stiffness level measured for $T_e/T_i = 1$ holds at all values of T_e/T_i and then extrapolating to $q_i^{GB} = 0$ applying equation (1), as shown in figure 3. This procedure yields the green full circles in figures 3 and 5.

The LH discharges were performed in slightly different experimental conditions. Therefore it can not be assumed that the ion temperature profiles are characterized by the same stiffness of the ICRH shots, since the power LH alters the q profiles due to current drive. To obtain the slope of the curve q_i^{GB} versus R/L_{Ti} in this case, q_i^{GB} and R/L_{Ti} were measured at the beginning and at the end of a small NBI blip: in this way we have obtained two points corresponding to the same discharge, one for plasma without NBI power and the other for plasma with some NBI power, from which, being the associated variation in rotation very small, an attempt to extrapolate the slope of the curve can be made. The threshold derived in this way is shown in figure 4 and also as violet full rhombi in 5 together with the thresholds of the ICRH set. The thresholds of the LH set are of course affected by much larger uncertainties, nevertheless they align quite well with the ICRH set in 5 .

For the low rotation shots figure 5 indicates a variation $\Delta R/L_{Ti} \approx 1.5$ for $1 < T_e/T_i < 2.4$. The dependence of the ITG threshold on T_e/T_i for $R/L_{Ti} > 1$ turns out to be rather weak, and this result reassures that the performance of ITER will not be severely hindered if the strong electron heating leads to exceeding the value $T_e/T_i = 1$.

3. MODELLING AND COMPARISON WITH EXPERIMENTS

For the low rotation dataset comparisons with analytical models and linear gyro-kinetic simulations were carried out, for the electrostatic case, both with adiabatic and kinetic electrons.

3.1 ANALYTICAL MODELS

Gyro-kinetic and fluid theories have been widely used for deriving analytical threshold expressions of electrostatic ITG modes. Significant references are the Romanelli's gyrokinetic formula proposed in [12] which for the case of adiabatic electrons and in the at density limit ($R/L_n < 2(1+ T_i/T_e)$ with R/L_n inverse density gradient length) is written as

$$\frac{R}{L_{Ti\ crit}} = \frac{4}{3}\left(1 + \frac{T_i}{T_e}\right) \cdot \left(1 + 2\frac{s}{q}\right), \tag{2}$$

and the Weiland reactive two- fluids model [13], which accounts for the influence and interactions of convection, compression, and thermalization of the species. A complete expression for the ITG threshold by theWeiland model in the at density limit ($R/L_n < 2$) is the following

$$\frac{R}{L_{Ti\ crit}} = \frac{R}{L_n}\left(\frac{2}{3} - \frac{1}{2}\frac{T_e}{T_i} + \frac{1}{8}\frac{T_e}{T_i}\frac{R}{L_n}\right) + \frac{1}{2}\frac{T_e}{T_i} + \frac{20}{9}\frac{T_i}{T_e}. \tag{3}$$

The comparison with the threshold values obtained from the experimental results of section 2 is shown in figure 6. Full circles and rhombi refer to the threshold values of figure 5, the lines are obtained by the formulas (2) and (3) with values of s/q and R/L_n characteristic of the discharges considered. Equation (2) yields somewhat higher values, but a similar trend with T_e/T_i. R/L_n at $\rho_{tor} = 0.33$ is comprised between 1.2 and 2.5 in these plasmas, so the at density limit of equation (2) is always satisfied. However, it is generally found that equation (2) agrees better with experiment and with linear gyro-kinetics when $s/q < 0.3$, and tends to overestimate the threshold for higher s/q [20]. In other words, (2) exhibits a too strong dependence on s/q, whilst the dependence on T_e/T_i is in agreement with data. The prediction of the Weiland model for the ITG threshold is in agreement with the values of the threshold measured by the experiments. As mentioned above, the stronger dependence predicted for $T_e/T_i < 1$ cannot be explored experimentally in the absence of rotation.

3.2 GKW LINEAR SIMULATIONS

Modelling using GKW [24] [25] has been performed. For the low rotation dataset linear electrostatic gyro-kinetic simulations were carried out, both with adiabatic and kinetic electrons.

The model allows the determination of the growth rate of the most unstable ITG mode. The GKW calculations of the dependences of the ITG growth rate with respect to T_e/T_i and R/L_{T_i} have been performed with parameters taken at $\rho_{tor} = 0.33$, in particular with s/q = 0.7/1.67 (=0.42), $n_e = 2.39 \times 10^{19}$ m^{-3}, $R/L_n = 1{:}95$ and $R/L_{T_i} = 6.4$.

Figures 7 and 8 show that at constant T_e/T_i, as expected, ITGs feature a threshold in R/L_{T_i} above which the growth rate γ increases. We can see also that the threshold decreases with increasing T_e/T_i and, as a consequence, at constant R/L_{T_i}, increasing T_e/T_i induces an increase of the growth rate.

The values of the threshold are obtained performing a parabolic fit for the curve γ versus R/L_{T_i} at each T_e/T_i and then by extrapolation to $\gamma = 0$. The results for the T_e/T_i scan are shown in figure 9.

The agreement between data and linear predictions is satisfactory in the range of T_e/T_i explored,

conrming a weaker trend for increasing T_e/T_i.

CONCLUSIONS

Experiments have been carried out in JET to explore the T_e/T_i dependence in ITER relevant range of parameters ($T_e/T_i \approx 1\text{-}1.6$) using low rotation plasmas with ICRH and LH to avoid the coupling of the effects of T_e/T_i and rotation which affected previous experiments. The new experimental result has found good agreement with theoretical predictions, for which two analytical models (Romanelli, Weiland) and the gyro-kinetic code GKW in linear mode have been used expanding the interval of T_e/T_i compared to previous studies. The latter allows for a more complete treatment of the complex phenomenon of ITG turbulence. The two analytical models provide directly analytical expressions of the ITG threshold as a function of various plasma parameters, and allow a direct comparison with experimental measurement. GKW instead allows the calculation of the linear growth rate of the drift wave, and then the reconstruction of the curve versus R/L_{T_i}, from which the threshold value can be extrapolated at $\gamma = 0$. The simulations were carried out at first in the case of adiabatic response of electrons and then considering the dynamics of electrons by treating them as kinetic species. A rather mild decrease of threshold with increasing T_e/T_i in the interval of ITER interest was found. The measurements agree well with theory predictions of ITG threshold from Weiland model and from linear GKW simulations, which represents a validation of linear gyro-kinetic theory in the range $T_e/T_i > 1$ of interest for ITER. The theoretical prediction also shows a stronger dependence in the range $T_e/T_i < 1$, allowing to resolve the apparent discrepancy of the new results with previous experiments, which, besides being compromised by the presence of rotation, were performed in the range $T_e/T_i < 1$ and as such not could be directly extrapolated to the ITER regimes. The validation of theory allows its reliable use for predicting ITER thresholds.

ACKNOWLEDGMENTS

The authors would like to thank A.G. Peeters, Y. Camenen, F.J. Casson, W.A. Hornsby, A.P. Snodin, D. Strintzi and G. Szepesi for making available the GKW code. This work is supported by the European Communities under the contract of Association EURATOM/ENEA-CNR, was carried out within EFDA. The views and opinions expressed herein do not necessarily reflect those of the European Commission.

REFERENCES

[1]. Petty C.C et al. 1999 Physical Review Letters **83** 3661
[2]. Suttrop W. et al. 2001 Europhys. Conference Abstract A **25** 989
[3]. Asp E et al. 2005 Plasma Physics and Controlled Fusion **47** 505
[4]. Manini A et al. 2004 Plasma Physics and Controlled Fusion **46** 1723
[5]. Manini A et al. 2006 Nuclear Fusion **46** 1047
[6]. Van Eester D et al. 2009 Plasma Physics and Controlled Fusion **51** 044007
[7]. Mattor N et al. 1988 Physics of Fluids **31** 1180

[8]. Romanelli F et al. 1989 Physics of Fluids **1** 1018
[9]. J.W. Connor and H.R. Wilson 1994 Plasma Physics and Controlled Fusion **36** 719
[10]. Kotschenreuther M et al. 1995 Physics of Plasmas **2** 2381
[11]. Hahm T.S and Tang W.M 1989 Physics of Fluid B **1** 1185
[12]. Guo S.C and Romanelli F 1993 Physics of Fluid B **5** 520
[13]. Weiland J 2000 Collective modes in inhomogeneous plasma (Bristol: Institute of Physics Publishing).
[14]. Weiland J et al. 2005 Plasma Physics and Controlled Fusion **47** 441
[15]. Casati A et al. 2008 Physics of Plasmas **15** 042310
[16]. Waltz R.E et al. 1994 Physics of Plasmas **1** 2229
[17]. 2008 Special Issue on Joint European Torus (JET) Fusion Science and Technology **53** 86101227
[18]. Giroud C.E. et al. 2008 Review of Scientific Instruments **79** 10F525
[19]. Mantica P et al. 2009 Physical Review Letters **102** 175002
[20]. Mantica P et al. 2011 Plasma Physics and Controlled Fusion **53** 124033
[21]. Garbet X et al. 2004 Plasma Physics and Controlled Fusion **46** 1351
[22]. Eriksson L.G et al. 1993 Nuclear Fusion **33** 1037
[23]. Challis C.D et al. 1989 Nuclear Fusion **29** 563
[24]. Peeters A.G et al. 2007 Physical Review Letters **98** 265003
[25]. Peeters A.G et al. 2009 Computer Physics Communication **180** 2650

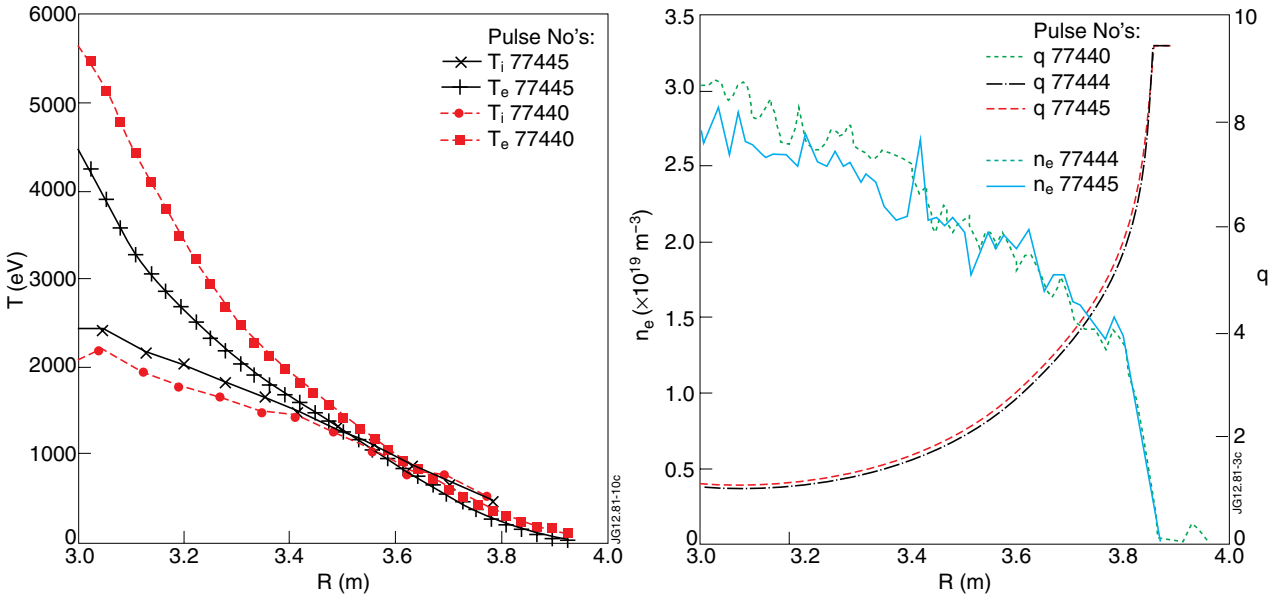

(a) Ion and electron temperature radial profiles: Pulse No's: 77445 ($He^3/n_{e0} \approx 5\%$, $T_e/T_i = 1.12$ at $\rho_{tor} = 0.33$) and 77440 ($H/n_{e0} \approx 5\%$, $T_e/T_i = 1.57$ at $\rho_{tor} = 0.33$).

(b) Electron density (n_e) and safety factor (q) radial proles. The graph shows that the scans of T_e/T_i were carried out at similar q and ne radial profiles.

Figure 1: Radial proles of ion and electron temperature, electron density and safety factor for representative discharges.

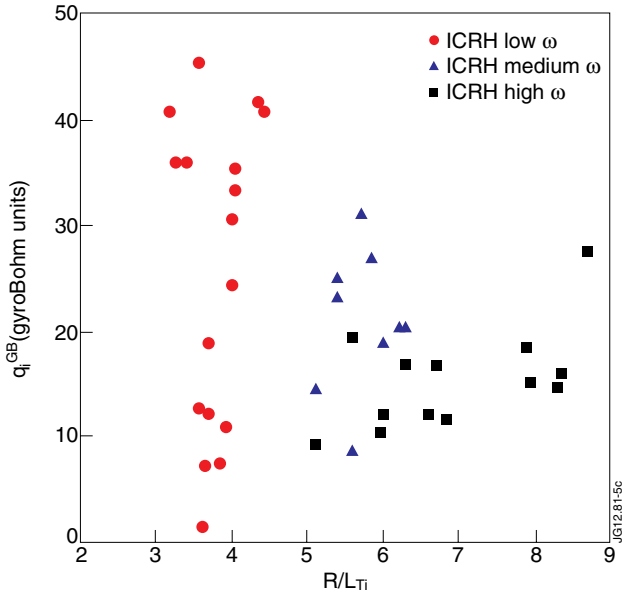

Figure 2: q_i^{GB} versus R/L_{T_i} at ρ_{tor} = 0.33 for the ICRH shots at dierent rotation levels.

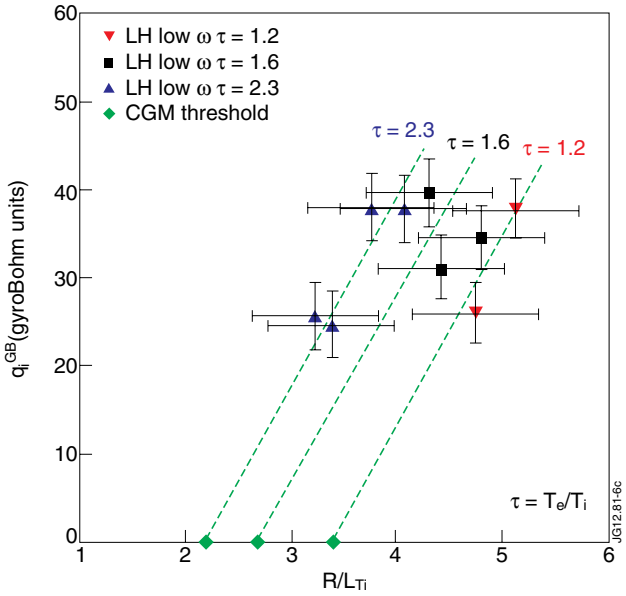

Figure 3: q_i^{GB} versus R/L_{T_i} at ρ_{tor} =for the ICRH shots at low rotation levels. The dashed lines are CGM ts of the T_e/T_i = 1.0 data, translated in R/L_{T_i} in order to deduce the threshold values (green full circles) at different $\tau = T_e/T_i$ by an extrapolation to $q_i^{GB} = 0$.

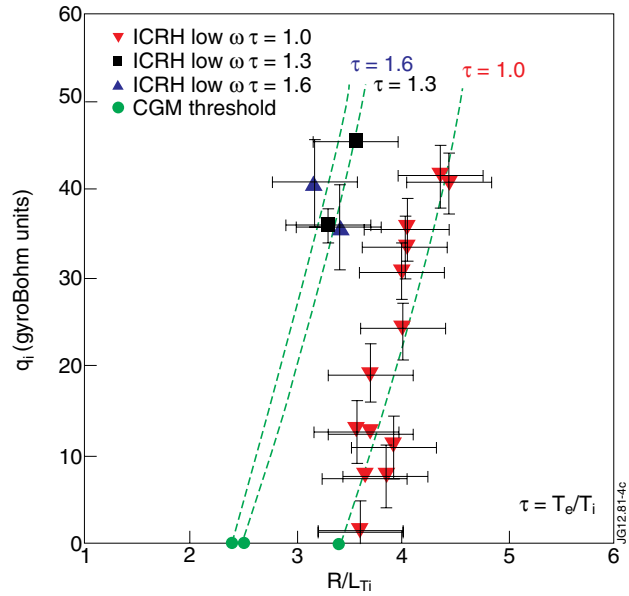

Figure 4: q_i^{GB} versus R/L_{T_i} at ρ_{tor} = for the LH shots at low rotation level. The dashed lines are CGM ts of the T_e/T_i = 1.2 data, translated in R/L_{T_i} in order to deduce the threshold values (violet full rhombi) at different $\tau = T_e/T_i$ by an extrapolation to $q_i^{GB} = 0$.

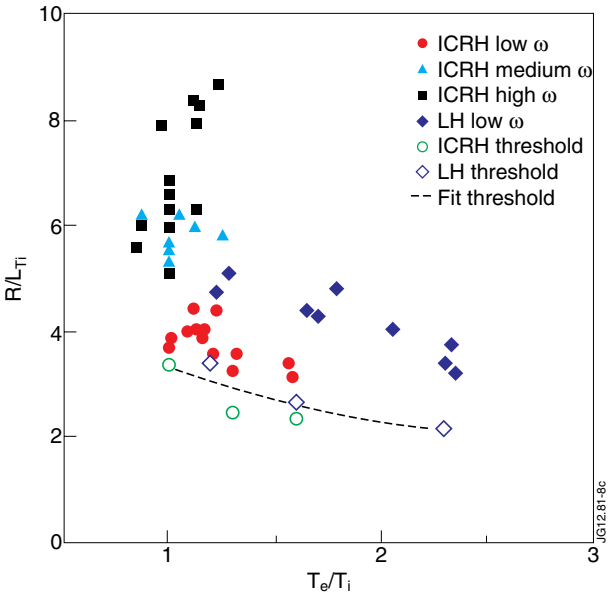

Figure 5: R/L_{T_i} versus T_e/T_i at ρ_{tor} =0.33 at different rotation levels. Black squares, blue triangles, red circles and small violet rhombi are actual R/L_{T_i}, green circles and violet big rhombi are extrapolations to $q_i^{GB} = 0$ as indicated in gures 3 and 4. The dashed line is a power fit performed on the threshold values.

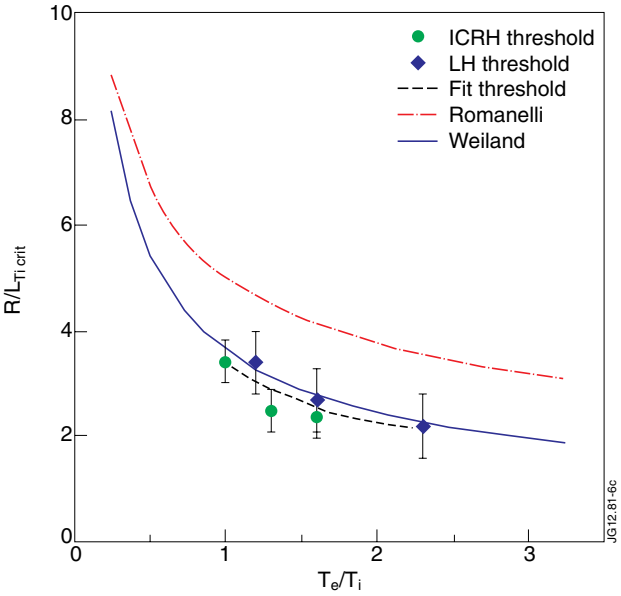

Figure 6: R/L_{T_i} versus T_e/T_i. Green circles and violet rhombi are the threshold values from figure 5. The blue and red lines are respectively after equations (2) with $s/q = 0.42$ and (3) with $R/L_n = 1.95$.

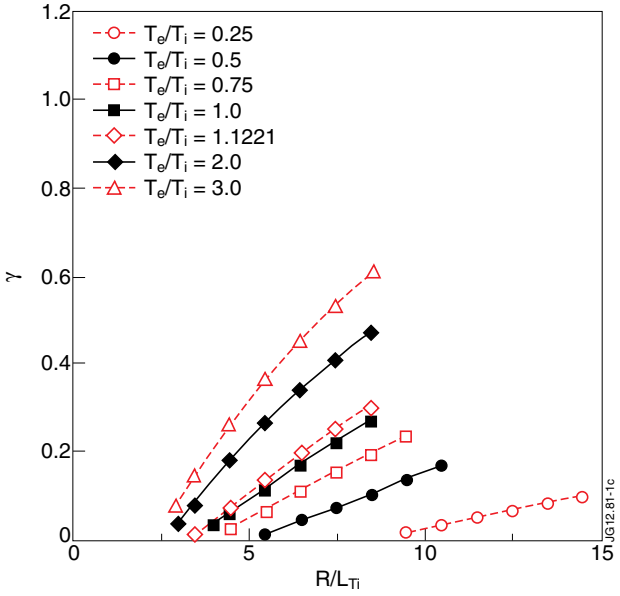

Figure 7: Numerical calculation with GKW of γ versus R/L_{T_i} for adiabatic electrons. Each curve corresponds to a different value of T_e/T_i and is obtained by a scan in R/L_{T_i} keeping the other plasma parameters fixed.

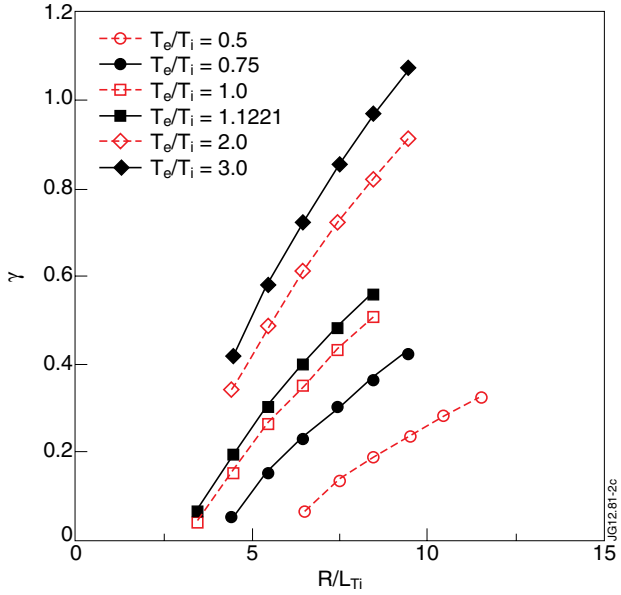

Figure 8: Numerical calculation with GKW of γ versus R/L_{T_i} for kinetic electrons. Each curve corresponds to a dierent value of T_e/T_i and is obtained by a scan in R/L_{T_i} keeping the other plasma parameters xed.

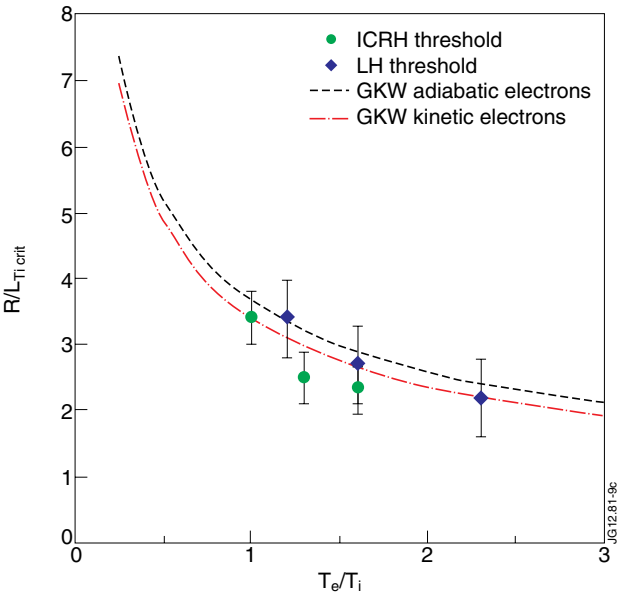

Figure 9: $R/L_{T_{icrit}}$ versus T_e/T_i. Green circles and violet rhombi are the threshold values of figure 5. The lines are the results of GKW linear simulations with adiabatic (black line) and kinetic electrons (red line).